# 基于多频外差原理的相位校正方法研究

郭创为[1,2,3], 王　阳[4], 邹文哲[2,3], 管钰晴[2,3], 张玉杰[1,2,3], 刘丽琴[2,3], 高志山[1], 雷李华[2,3*]

(1. 南京理工大学 电子工程与光电技术学院，江苏 南京 210094；
2. 上海市计量测试技术研究院，上海 201203；
3. 上海市在线检测与控制技术重点实验室，上海 201203；
4. 中国合格评定国家认可中心 北京 100062)

**摘　要：**相位测量轮廓术因其简单低廉的特点被广泛用于光学三维测量领域，高精度的相位获取是测量的关键步骤。多频外差是相位测量轮廓术中常用的解包裹相位算法，针对多频外差解相位后产生的相位跳跃性误差，提出一种基于多频外差原理的相位校正方法。利用传统相移法和多频外差求出包裹相位和展开相位，针对展开相位中出现的跳跃性误差，通过展开相位对误差产生原因和误差位置进行初步确定，将多个频率的包裹相位进行对比，确定误差是否真实存在，对出现误差的像素点进行修正得到新的展开相位。实验结果表明：在对表面形状规则的物体测试时，展开相位光滑无跳跃性误差，表面三维重建无异常凹凸区域，实现了对解相位中跳跃性误差的消除，验证了该校正方法的有效性。

**关键词：**误差校正；　多频外差；　展开相位；　跳跃性误差

**中图分类号：**TP391.4; TH741　　**文献标志码：**A　　**DOI：**10.3788/IRLA20220697

## 0　引　言

结构光三维测量技术是目前主流的三维测量方法，其具有非接触式测量、成像精度高、重构速度快等优点，被广泛地应用于工业自动检测、逆向工程、人体测量、航天航空等领域[1−3]。其基本原理是通过向被测元件投射结构光，采集经被测元件调制的图像，根据解算图像中的包裹相位得到被测元件的表面相位分布，由此实现面形重构。相位解算的精度将直接影响到物体最终的重构精度，所以在结构光三维测量中选用高精度标定方法[4]和相位解算方法十分重要。

相移法是最常用的相位测量方法，但通过相移法得到的是包裹相位，其范围在 (0,2π]，需要对包裹相位进行解包裹计算才能得到真实的相位分布。相位解包裹方法主要可分为空间相位解包裹和时间相位解包裹两大类[5−8]。空间相位解包裹只需任意一幅不特定时刻的包裹相位图就可以计算出绝对相位，但是该方法只能用于表面光滑且轮廓简单的物体，并且还要满足高信噪比的前提条件[9−12]，这一系列的要求制约了空间相位解包裹的应用场景。

空间相位解包裹的本质是一种积分过程，任何一点的误差都会随展开过程演变成累积误差[13]。时间相位解包裹需要投影多个频率不同时刻的条纹图以确定绝对相位，相比空间相位解包裹，该方法每个像素点的相位是在时间轴上展开得到的，在空间上彼此孤立，展开过程不依靠展开路径和相邻相位信息避免了误差的传递。同时，时间相位解包裹方法具有展开结果稳定、过程简单、不会受到待测物体形貌复杂程度的影响等优点[14]。

多频外差解包裹作为最常用的时间相位解包裹算法，具有原理简单、解算精度高等优点。但在实际测量中，由于测量环境、物体表面特性、相机和投影仪的非线性误差等因素，在条纹级数取整过程会出现

**收稿日期：**2023−01−20；　**修订日期：**2023−02−25

**基金项目：**上海市 2021 年度“科技创新行动计划”自然科学基金 (21ZR1483100)

**作者简介：**郭创为，男，硕士生，主要从事光学三维成像方面的研究。

**导师简介：**高志山，男，教授，博士，主要从事精密光学测试技术和先进光学设计方面的研究。

**通讯作者：**雷李华，男，高级工程师，博士，主要从事微纳米计量技术方面的研究。

错误取整导致跳跃性误差的产生，因此使用多频外差方法时必须设法修正跳跃性误差。Cai 等[15] 利用 Hilbert 算法对相位误差进行补偿，对连续表面测量效果显著，但测量效率较低。雷志辉等[16] 经过对多频外差原理的改进提出利用双频投影条纹的叠栅特性进行解包裹的方法，但该方法仅对双频外差法中出现的跳跃误差有效，对多频外差法效果并不理想。陈松林等[17] 对雷志辉等人的方法加以改进，最终得到平滑无跳变的解包裹相位，但该方法对投影条纹有诸多约束条件，限制了条纹投影的灵活性。陈玲等[18] 对多频外差解相后的展开相位进行分析，使用邻域像素点对误差处进行修正，但是大邻域的选取降低了条纹投影的分辨率且无法精准判断相位跳跃产生原因。

文中对多频外差解包裹原理进行了充分研究，对所得展开相位中跳跃性误差的产生原因进行了深入的分析讨论，提出一种多频外差相位校正方法，对由多频外差法解得的展开相位进行误差校正，并将校正前后的展开相位进行比较。

## 1 原理实验分析

### 1.1 多频外差解包裹相位原理与误差分析

多频外差解包裹相位指将多个不同频率的条纹图像进行叠加，通过对叠加在一起的包裹相位进行求解，得到各个频率的绝对相位。最常用的多频外差解包裹方法是双频外差和三频外差。

#### 1.1.1 双频外差原理及相位误差分析

双频外差原理如图 1 所示，向待测物体表面投射条纹节距分别为$p_1$, $p_2$的两种正弦条纹图，为方便后续计算此处应保证$p_1 < p_2$，叠加后形成节距为$p_{12}$的叠栅，对物体上任意一点，设其水平方向坐标为$x$，对应的条纹级次分别为$n_1$、$n_2$，则成立以下等式：

$$x = p_1 n_1 = p_2 n_2 \tag{1}$$

$$\Delta n_i = \frac{\phi_i}{2\pi}, \Delta n_i \in [0,1), i = 1,2 \tag{2}$$

$$n_t = N_t + \Delta n_i, N_t \in Z \tag{3}$$

$$p_{12} = \frac{p_1 p_2}{p_2 - p_1} \tag{4}$$

式中：$N_i$代表条纹级次的整数部分；$\Delta n_i$代表条纹级次的小数部分；$\phi_i$代表对应条纹的包裹相位。

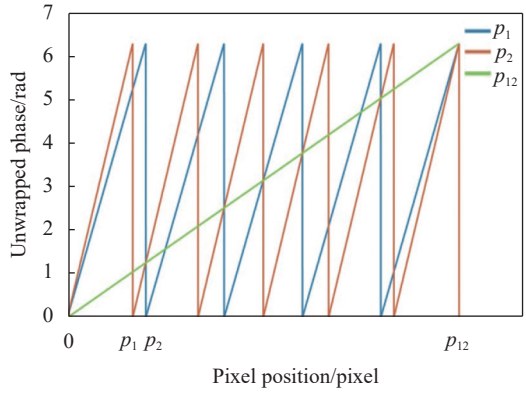


图 1 双频外差原理

Fig.1 Dual frequency heterodyne principle

先以简单的双频外差为例分析其原理及误差产生原因，由公式 (1) 可推出：

$$n_t = \frac{p_i (n_1 - n_2)}{p_2 - p_1} \quad i = 1,2 \tag{5}$$

将公式 (3) 代入功能等式 (5) 中，可得：

$$n_1 = \frac{p_2 (n_1 - n_2)}{p_2 - p_1} = \frac{p_2 (N_1 - N_2 + \Delta n_1 - \Delta n_2)}{p_2 - p_1} \tag{6}$$

$$n_2 = \frac{p_1 (n_1 - n_2)}{p_2 - p_1} = \frac{p_1 (N_1 - N_2 + \Delta n_1 - \Delta n_2)}{p_2 - p_1} \tag{7}$$

$$N_1 - N_2 = \begin{cases} \dfrac{p_2 - p_1}{p_1} n_2 + \Delta n_2 - \Delta n_1 \\ \dfrac{p_2 - p_1}{p_2} n_1 + \Delta n_2 - \Delta n_1 \end{cases} \tag{8}$$

对于上述公式 (6)~(8)，由于$p_1$、$p_2$已知，$\Delta n_1$、$\Delta n_2$可由公式 (2) 求得。故若能解出$N_1 - N_2$的值，便可求出$n_1$、$n_2$。将展开后的绝对相位命为$\varphi_i$，则可将绝对相位与包裹相位的关系表示为：

$$\varphi_i = 2\pi n_i = 2\pi N_i + \phi_i \tag{9}$$

下面分析误差的产生原因，先假设采集到的图像上的某点水平方向坐标为$x$，该点在$[m, m+1)$级叠栅条纹中，即$n_{12} \in [m, m+1), N_{12} = m$，结合公式 (4) 有：$x \in \left[\dfrac{m p_1 p_2}{p_2 - p_1}, \dfrac{(m+1) p_1 p_2}{p_2 - p_1}\right)$。

故公式 (8) 可写为：

$$N_1 - N_2 \in [m + \Delta n_2 - \Delta n_1, (m+1) + \Delta n_2 - \Delta n_1) \tag{10}$$

已知$\Delta n_1, \Delta n_2 \in [0,1)$，所以$\Delta n_2 - \Delta n_1 \in [-1,1)$，结合$N_i \in Z$，公式 (10) 可改写为：

$$N_1 - N_2 = \{m, m+1\} \tag{11}$$

设$N_1 - N_2 = k$，结合公式 (11) 对公式 (10) 分情况

讨论, 可得:

$$\begin{cases} \phi_2-\phi_1>0, N_1-N_2=k=m+1 \\ \phi_2-\phi_1\leqslant 0, N_1-N_2=k=m \end{cases} \tag{12}$$

结合公式 (6)、(7)、(9), $\varphi_i$可表示为:

$$\begin{cases} \varphi_1=\dfrac{p_2[2\pi k+(\phi_1-\phi_2)]}{p_2-p_1} \\ \varphi_2=\dfrac{p_1[2\pi k+(\phi_1-\phi_2)]}{p_2-p_1} \end{cases} \tag{13}$$

在实际图像中, 由于相邻像素点受环境中各类噪声影响, 可能造成某一点处$\phi_1-\phi_2$出现 2π 误差, 在公式 (13) 中可以看到, 该误差在因子$p_1/(p_2-p_1)$, $p_2/(p_2-p_1)$的作用下被放大。

结合公式 (9) 将条纹级数整数部分和小数部分分开计算:

$$\begin{cases} \varphi_1=2\pi floor\left\{\dfrac{p_2\left[k+\dfrac{\phi_1-\phi_2}{2\pi}\right]}{p_2-p_1}\right\}+\phi_1 \\ \varphi_2=2\pi floor\left\{\dfrac{p_1\left[k+\dfrac{\phi_1-\phi_2}{2\pi}\right]}{p_2-p_1}\right\}+\phi_2 \end{cases} \tag{14}$$

式中: $floor\{\}$表示向下进行取整。通过公式 (14) 可以将误差放大因子$p_1/(p_2-p_1)$, $p_2/(p_2-p_1)$去除, 此时剩余误差项$\phi_1,\phi_2$。

1.1.2 三频外差原理

向物体投射三种不同节距的正弦条纹图, 节距分别为$p_1,p_2,p_3$, $p_1$和$p_2$叠加形成节距为$p_{12}$的叠栅, 同理$p_2$和$p_3$叠加形成节距为$p_{23}$的叠栅, 将$p_{12}$和$p_{23}$叠加形成节距为$p_{123}$的叠栅, 注意应保证$p_1<p_2<p_3$, 原理与双频外差相同。则:

$$p_{123}=\frac{p_{12}p_{23}}{p_{23}-p_{12}}=\frac{p_1p_2p_3}{p_{12}+p_{23}-2p_{13}} \tag{15}$$

根据待测物体尺寸确定条纹投影范围, 需满足待测物体在投影中心区域且被投影的条纹完全覆盖。由公式 (15) 可以计算出叠栅节距$p_{123}$, 当$p_{123}$略大于投影仪分辨率时, 叠栅$p_{123}$刚好能够覆盖整个视场, 较为接近投影仪横向分辨率, 视场内$p_{123}$不足一个周期, 即$n_{123}<1, N_{123}=0, n_{123}=\Delta n_{123}$。由已经推导过的双频外差原理可知:

$$\begin{cases} N_{12}=floor\left\{\dfrac{p_{23}\left[r+\dfrac{\phi_{12}-\phi_{28}}{2\pi}\right]}{p_{23}-p_{12}}\right\} \\ N_{23}=floor\left\{\dfrac{p_{12}\left[r+\dfrac{\phi_{12}-\phi_{22}}{2\pi}\right]}{p_{29}-p_{12}}\right\} \end{cases} \tag{16}$$

$$\begin{cases} \varphi_{12}=2\pi floor\left\{\dfrac{p_{23}\left[r+\dfrac{\phi_{12}-\phi_{23}}{2\pi}\right]}{p_{23}-p_{12}}\right\}+\phi_{12} \\ \varphi_{23}=2\pi floor\left\{\dfrac{p_{12}\left[r+\dfrac{\phi_{12}-\phi_{23}}{2\pi}\right]}{p_{23}-p_{12}}\right\}+\phi_{23} \end{cases} \tag{17}$$

公式 (16)、(17) 中$r=N_{12}-N_{23}$, $N_{123}=0$, 故

$$r=\begin{cases} 1, \phi_{23}-\phi_{12}>0 \\ 0, \phi_{23}-\phi_{12}\leqslant 0 \end{cases} \tag{18}$$

由公式 (17) 可求出绝对相位$\varphi_{12},\varphi_{23}$, 反推可得$N_{12},N_{23}$, 再由公式 (14) 可解出$\varphi_1,\varphi_2,\varphi_3$。

### 1.2 展开相位误差分析及修正方法

由上文推导可知, 误差主要有两种, 受测试环境、系统硬件 (相机、投影仪) 精度影响, 使得条纹整数级$N_{12}(N_{23})$取整错误, 如导致$N'_{12}=N_{12}+1$, 这就会在展开相位$\varphi_1$中发生幅值为$floor\{p_2/(p_2-p_1)\}\times 2\pi$的跳跃性误差, $(\phi_1-\phi_2)/2\pi$的误差值也会对展开相位造成幅值为 2π 的相位误差。

1.2.1 相位展开误差修正方法

(1) 采集光栅投影后的图像, 利用相移法求解出$p_1,p_2,p_3$的包裹相位, 利用多频外差原理求解展开相位$\varphi_1,\varphi_2,\varphi_3$;

(2) 通过后一像素点相位幅值减当前像素点相位幅值计算展开相位的梯度, 找出$\varphi_i(i=1,2,3)$中可能存在误差的可疑点, 根据误差的幅值判断误差来源于$N_{12}(N_{23})$或$\phi_i(i=1,2,3)$并确定误差的起始和终止像素点位置 (连续误差像素点一般小于 5 个), 确定来源于$N_{12}(N_{23})$后抹除跳跃性误差并对跳跃点处加以平滑;

(3) 误差来源$\phi_i$时, 通过对邻域像素点计算梯度确定误差的起始和终止像素点位置 (连续误差像素点一般小于 5 个), 判断该点处$\phi_1,\phi_2,\phi_3$是否都发生相位突变, 如果 3 个频率的展开相位在该点都有相位突变, 则证明此处为物体表面的真实结构, 在投影条纹的两

侧会出现$\varphi_1 \approx \varphi_2 \approx \varphi_3$的情况，投影时两侧条纹不属于测量区，故不作考虑；

(4) 如果 3 个频率中有 2 个的展开相位在该点区域都有相位突变，则需要分情况讨论，如果有相位变化的两个展开相位在此点处的包裹相位值非常接近，(此处阈值设为 π/10)，认为此处属于相位误差，对该点进行±2π的修正，若此处两包裹相位值大于 π/10，认为该区域解相正确；若仅有 1 个展开相位有相位突变，则认为此处属于解相位错误。

以$\varphi_1$为例进行流程演示，设$a$点为当前待检测像素点，$b$点为$a$点水平方向下一像素点，$m = floor\{b+1, b+5\}$，$n = m-1$，具体流程图如图 2 所示。

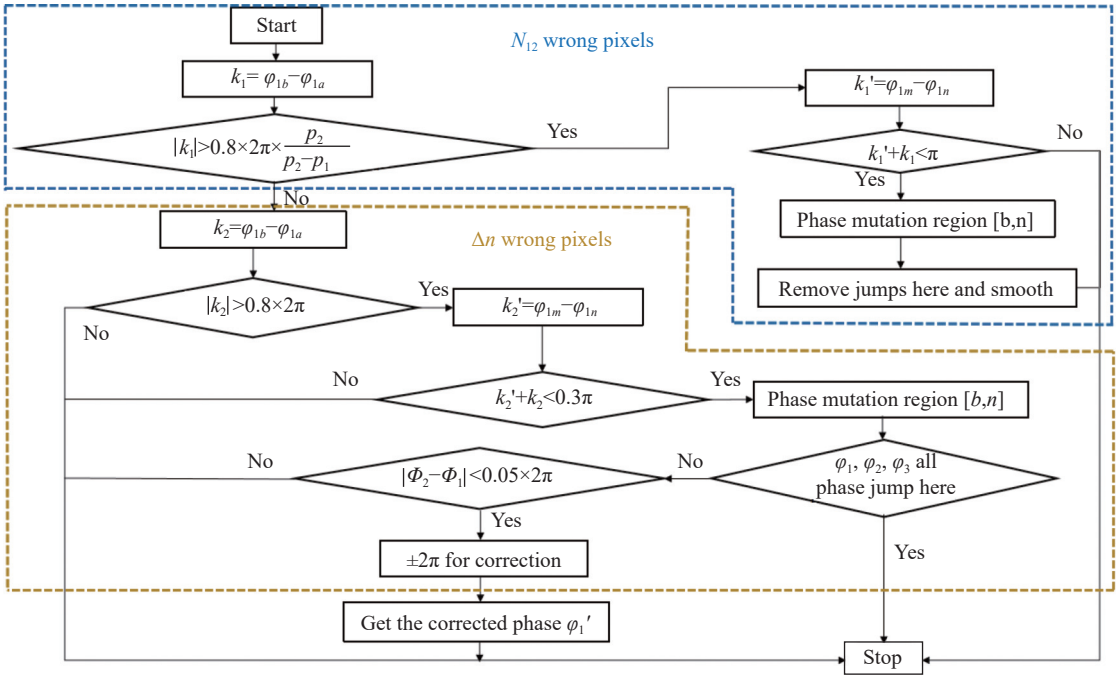


图 2 误差校正流程图

Fig.2 Error correction flow chart

### 1.3 实验分析

验证文中方法的有效性，对标准球进行三维测量。首先搭建三维测量系统，利用张正友标定法对系统进行标定。该实验使用 basler a2A1920 工业相机，分辨率为 1 920 pixel×1 080 pixel，使用 XGIMI 公司 XG14V 型号投影仪，分辨率为 1 920 pixel×1 080 pixel，实验采集图像如图 3 所示。

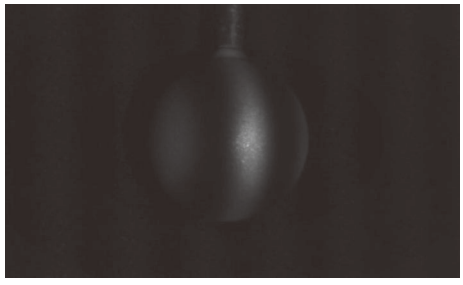

图 3 实验采集图像

Fig.3 Images acquired in the experiment

实验采用三频外差、四步相移的方案，投影$p_1 = 24, p_2 = 26, p_3 = 28$的光栅条纹。利用参考文献[16]提出的改进后多频外差解包裹方法，对相机采集到的实验条纹图进行解包裹相位处理，得到展开相位$\varphi_1, \varphi_2, \varphi_3$，其中$\varphi_1$相位分布如图 4(a) 所示，可以明显观察到由展开相位幅值突变引起的带状错误解相位区域，其中包含由$(\phi_1-\phi_2)/2\pi$的误差引起的幅值为 2π 的相位突变以及由条纹整数级次$N_{12}$取整错误引起的幅值为$floor\{p_2/(p_2-p_1)\}\times2\pi$的相位突变。为精确确定展开相位误差的产生原因和误差所在像素点的位置，随机取$\varphi_1$展开相位图的某一行进行观察分析，这里取展开相位$\varphi_1$的第 470 行进行观察，如图 4(b) 所示，在第 450 个像素点和第 475 个像素点附近区域出现幅值约为 2π 的相位突变，证明在这两个区域内的像素点相位解包裹过程中由于$\phi_i$的误差造成了错误的解相，在第 504、505 pixel 点处，相位出现了幅值

较大的跳跃性误差，证明此区域内$N_{12}$的取值发生错误，由$p_1=24, p_2=26$知，由$N_{12}$错误取值导致的相位误差理论值为26π，实际由于环境噪声及其他因素，实际相位幅值误差为24.2π。图5所示为展开相位$\varphi_{12}$的整数级次$N_{12}$，在与图4(b)相位发生跳跃性误差的对应像素点处，展开相位$\varphi_{12}$整数级次取整发生错误。

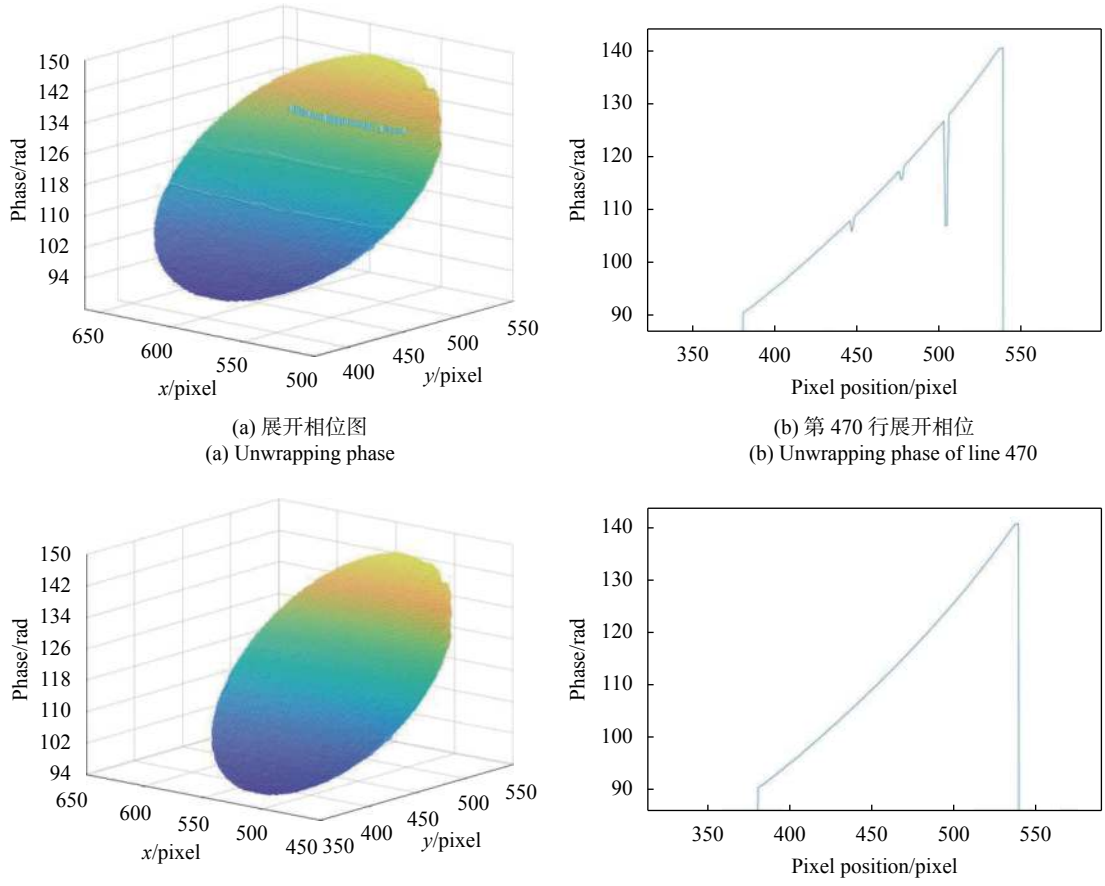


(a) 展开相位图
(a) Unwrapping phase

(b) 第 470 行展开相位
(b) Unwrapping phase of line 470

(c) 校正后展开相位图
(c) Corrected unwrapping phase

(d) 校正后第 470 行展开相位
(d) Unwrapping phase of line 470 after correction

图 4 校正前后展开相位分布

Fig.4 Unwrapping phase distribution before and after correction

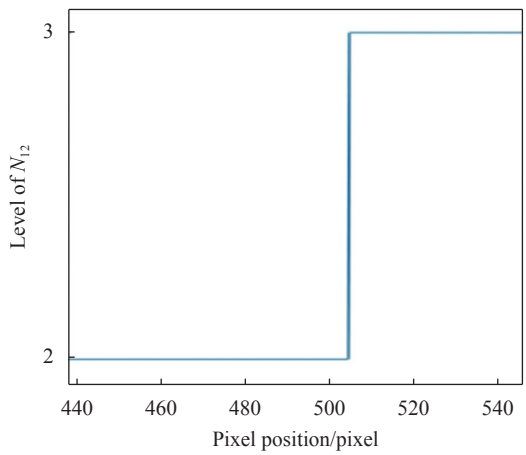


图 5 $\varphi_{12}$的整数级次$N_{12}$

Fig.5 Integer level $N_{12}$ of $\varphi_{12}$

使用文中提出的误差校正算法对所得展开相位进行误差校正，得到修正后展开相位$\varphi_1'$，相位分布如图4(c)所示，将图4(c)与图4(a)对比，可以观察到原相位分布图中出现的相位突变区域已被成功消除，相位误差被成功修复，取$\varphi_1'$第470行观察如图4(d)所示，对比图4(b)，原展开相位图在对应像素点位置出现的突变相位区域被成功修复，校正后的展开相位过渡平滑无相位突变现象。

为更加直观的观察校正前后测量效果，分别以修正前后的展开相位进行三维点云重建，结果如图6所示，图6(a)为相位修正前重建结果，图6(b)为相位修正后重建结果，在图6(a)中，可以观察到由解包裹相

位错误导致的表面残缺区域，对比图 6(b)，校正后的展开相位的三维点云重建中将解相位误差引起的表面突变很好的修复，得到的表面形貌平滑，无表面高度突变区域。

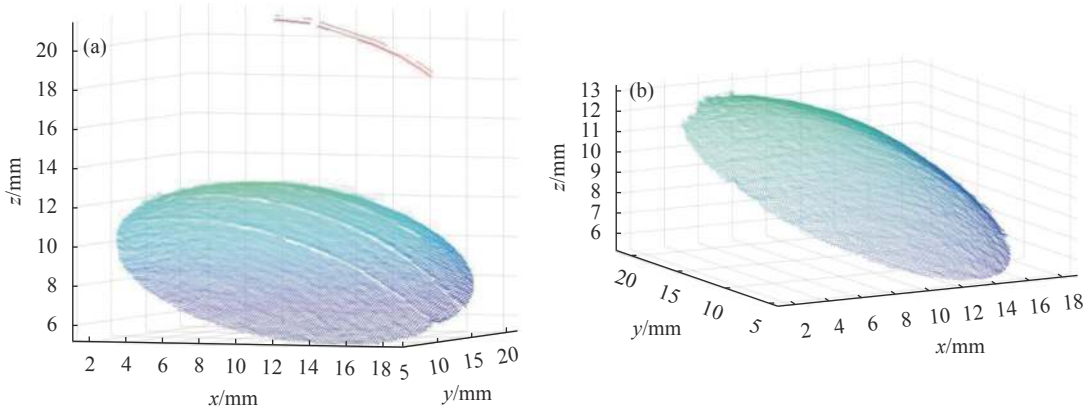


图 6 (a) 校正前三维点云图; (b) 校正后三维点云图

Fig.6 (a) 3D point cloud before correction; (b) 3D point cloud after correction

## 2 结 论

基于现有的多频外差解相位原理，在充分分析原理中跳跃性误差产生原因的基础上，提出了一种相位误差校正算法，针对引起误差的来源项$N_{12}$ ($N_{23}$)和$\Delta n$进行分析，通过多情况讨论确定误差类型并进行相位校正。实验结果表明，该方法可以精准定位误差产生区域并有效校正解包裹相位中产生的跳跃性误差，得到的展开相位平滑无跳变，三维点云重建无异常表面高度变化，验证了该校正方法的可行性。

**参考文献：**

[1] Fu Y J, Han Y H, Chen Y, et al. Research progress of 3D measurement technology based on phase coding [J]. ***Infrared and Laser Engineering***, 2020, 49(3): 0303010. (in Chinese)

[2] Susana Martínez-Pellitero, Eduardo Cuesta, Sara Giganto, et al. New procedure for qualification of structured light 3D scanners using an optical feature-based gauge [J]. ***Optics and Lasers in Engineering***, 2018, 110: 193-206.

[3] Liu D, Yan T L, Wang D D, et al. Review of fringe-projection profilometry and phase measuring deflectometry [J]. ***Infrared and Laser Engineering***, 2017, 46(9): 0917001. (in Chinese)

[4] Marrugo Andres G, Raul Vargas, Song Zhang, et al. Hybrid calibration method for improving 3D measurement accuracy of structured light systems[C]//Proceedings of SPIE, 2020, 11490, 1149008.

[5] Li Y, Zhang G H, Ma L H, et al. Review of dynamic three-dimensional surface imaging based on fringe projection [J]. ***Infrared and Laser Engineering***, 2020, 49(3): 0303005. (in Chinese)

[6] Liu L, Xi D D, Cheng L, et al. Enhanced gray-code method for three-dimensional shape measurement [J]. ***Infrared and Laser Engineering***, 2020, 49(11): 0303005.

[7] Wang B Y, Wang R, Zhang J S, et al. Dual-frequency phase unwrapping method for anti-jump errors of wrapped phase [J]. ***Integrated Ferroelectrics***, 2022, 226(1): 72-81.

[8] Wu H T, Cao Y P, An H H, et al. A novel phase-shifting profilometry to realize temporal phase unwrapping simultaneously with the least fringe patterns [J]. ***Optics and Lasers in Engineering***, 2022, 153: 107004.

[9] Liu F, Luo H F, Jiang H L, et al. Modified three-dimensional reconstruction based on three-frequency three-step phase shifting algorithm [J]. ***Infrared and Laser Engineering***, 2022, 51(4): 20210179. (in Chinese)

[10] Han X, Wang L, Fu Y J. Phase unwrapping method based on dual-frequency heterodyne combined with phase encoding [J]. ***Infrared and Laser Engineering***, 2019, 48(9): 0913003. (in Chinese)

[11] Lu L, Jia Z Y, Wu K, et al. 3D reconstruction of multi-target moving objects based on phase-shifting method [J]. ***Infrared and Laser Engineering***, 2020, 49(3): 0303011. (in Chinese)

[12] Wang Y W, Chen X C, Wang Y J. Modified dual-frequency geometric constraint fringe projection for 3D shape measurement [J]. ***Infrared and Laser Engineering***, 2020, 49(6): 20200049. (in Chinese)

[13] Han Y, Yang Y Z, Su X L. A phase unwrapping method based on multifrequency heterodyne [J]. ***Journal of Donghua University* (*Natural Science*)**, 2021, 47(5): 105-110, 127. (in Chinese)

[14] Han X. Research on 3D fringe projection measurement method based on time phase unwrapping[D]. Nanchang: Nanchang Hangkong University, 2019. (in Chinese)

[15] Cai Z W, Liu X L, Jiang H, et al. Flexible phase error compensation based on Hilbert transform in phase shifting profilometry. [J]. ***Optics Express***, 2015, 23(19): 25171-25181.

[16] Lei Z H, Li J B. Full automatic phase unwrapping method based on projected double spatial frequency fringes [J]. ***Acta Optica Sinica***, 2006, 26(1): 39-42. (in Chinese)

[17] Chen S L, Zhao J B, Xia R B. Improvement of Phase Unwrapping Method Based on Multi-Frequency Heterodyne Principle [J]. ***Acta Optica Sinica***, 2001, 6, 36(4): 155-165. (in Chinese)

[18] Chen L, Deng W Y, Lou X P. Phase unwrapping method based on multi-frequency interferometry [J]. ***Optical Technology***, 2012, 38(1): 73-78. (in Chinese)

# Study of phase correction method based on multi-frequency heterodyne principle

Guo Chuangwei[1,2,3], Wang Yang[4], Zou Wenzhe[2,3], Guan Yuqing[2,3], Zhang Yujie[1,2,3], Liu Liqin[2,3], Gao Zhishan[1], Lei Lihua[2,3*]

(1. School of Electronic and Optical Engineering, Nanjing University of Science and Technology, Nanjing 210094, China;
2. Shanghai Institute of Measurement and Testing Technology, Shanghai 201203, China;
3. Shanghai Key Laboratory of Online Test and Control Technology, Shanghai 201203, China;
4. China National Accreditation Service for Conformity Assessment, Beijing 100062, China)

**Abstract:**

**Objective** Phase Measurement Profilometry (PMP) has become the mainstream optical three-dimensional measurement method due to its advantages of high imaging accuracy and fast reconstruction speed. Phase Measurement Profilometry performs surface reconstruction through phase calculation of projected images. The accuracy of phase calculation largely determines the final three-dimensional reconstruction accuracy. Therefore, obtaining high-precision unwrapped phase is the key step of measurement. Multi-frequency heterodyne is a commonly used unwrapping phase algorithm in phase measurement profilometry. When unwrapping the wrapped phase, due to the influence of the measurement environment, the characteristics of the object surface, the nonlinear error of the camera and projector, and other factors, the fringe series will be incorrectly rounded, and the unwrapped phase will produce a jumping phase error. This jumping error will lead to the wrong concave and convex areas or burrs on the surface of the reconstructed object, which greatly affects the accuracy of 3D reconstruction. Therefore, it is necessary to study a correction method that can eliminate or compensate the jumping error. Thus, a phase correction method based on multi-frequency heterodyne principle is proposed.

**Methods** The specific flow of the phase correction method based on the principle of multi-frequency heterodyne is drawn (Fig.2). The initial wrapped phase and the unwrapped phase are calculated by using the traditional phase shift method and multi-frequency heterodyne. Because there are two different jumping errors in the unwrapped phase, the cause of the error and the error location are preliminarily determined by the gradient and amplitude of the unwrapped phase. By comparing the phase amplitude of multiple wrapped phases with different frequencies at the problem point, whether the error at the problem point really exists is determined. According to the principle of multi-frequency heterodyne, the error amplitude introduced by the error item is analyzed, and the pixel with the error is corrected to obtain a new unwrapped phase.

**Results and Discussions** Phase Measurement Profilometry is used to reconstruct the standard sphere in three dimensions, and the proposed phase correction method is used to correct the error of the unwrapped phase. By comparing the original unwrapped phase (Fig.4(a)) and the corrected unwrapped phase (Fig.4(c)), it can be observed that the phase mutation region in the original phase distribution map has been successfully eliminated and the phase error has been successfully repaired. The 470th line of the unwrapped phase before and after correction is observed (Fig.4(b) and Fig.4(d)). The abrupt phase area of the original unwrapped phase map at the corresponding pixel position has been successfully repaired. The corrected unwrapped phase transition is smooth without phase abrupt change. The point cloud reconstruction before and after correction is compared (Fig.6), the surface defect area caused by unwrapping phase error has been well repaired.

**Conclusions** In view of the jumping error in the existing multi-frequency heterodyne phase demodulation process, a phase error correction algorithm is proposed based on the full analysis of the reasons for the jumping error in the principle. The principle of this method is simple and easy to implement, the error correction is accurate and the correction speed is fast. The source terms that cause the error are analyzed, the error type is determined and phase correction is carried out through multiple discussions. After correcting the standard sphere unwrapped phase of the traditional multi-frequency heterodyne measurement, all the jumping errors in the original unwrapped phase are corrected. The experimental results show that this method can accurately locate the cause and region of the jumping error and effectively correct the jumping error in the unwrapping phase. The unwrapped phase corrected by this method is smooth without jumping, and the 3D point cloud reconstruction surface has no abnormal concave and convex areas, which realizes the elimination of the jumping error in the unwrapping phase, and verifies the feasibility and effectiveness of this correction method.

**Key words:** error correction; multi-frequency heterodyne; unwrapping phase; jumping error

**Funding projects:** Shanghai 2021 "Science and Technology Innovation Action Plan" Natural Science Foundation (21ZR1483100)